Importance of the Roughness and Residual Stresses of Dental Implants on Fatigue and Osseointegration Behavior. In Vivo Study in Rabbits

Eugenio Velasco, PhD, MD, DDS[1]
Loreto Monsalve-Guil, PhD, MD, DDS[1]
Alvaro Jimenez, PhD, MD, DDS[1]
Iván Ortiz, PhD, MD, DDS[1]
Jesús Moreno-Muñoz, PhD, MD, DDS[1]
Enrique Nuñez-Marquez, PhD, MD, DDS[1]
Marta Pegueroles, PhD, MD, DDS, MMSc[2]
Román A. Pérez, PhD, MD, DDS, MMSc[3]
Francisco Javier Gil, PhD, MD, DDS, MMSc[3]*

This study focuses on the fatigue behavior and bone-implant attachment for the more usual surfaces of the different CP-titanium dental implants. The implants studied were: as-received (CTR), acid etching (AE), spark-anodization (SA), and with a grit-blasted surface (GB). Residual stresses were determined by means of X-ray diffraction. The fatigue tests were carried out at 37°C on 160 dental implants, and the stress-failure (S-N) curve was determined. The fatigue tests showed that the grit-blasting process improved fatigue life. This is a consequence of the layer of compressive residual stresses that the treatment generates in titanium surfaces. Further, our aim was to assess and compare the short- and midterm bone regenerative potential and mechanical retention of the implants in bone of New Zealand rabbits. The mechanical retention after 4 and 10 weeks of implantation was evaluated with histometric and pull-out tests, respectively, as a measure of the osseointegration of the implants. The results demonstrated that the GB treatment produced microrough that accelerated bone tissue regeneration and increased mechanical retention in the bone bed at short periods of implantation in comparison with all other implants tested. The GB surface produced an improvement in mechanical long-time behavior and improved bone growth. These types of treated implants can have great potential in clinical applications, as evidenced by the outcomes of the current study.

Key Words: Titanium, dental implants, fatigue resistance, shot blasting, residual stresses, osseointegration

INTRODUCTION

The clinical success of titanium dental implants is based on a strong and long-lasting connection between implant and bone tissue. For this purpose, dental implants are designed with specific features that trigger cellular actions, thereby enhancing the proper integration of the dental implant with the surrounding bone. For instance, the stiffness, wettability, or surface roughness (among other parameters) are critical in promoting these cellular activities. In the dental implant field, roughness is considered as one of the most relevant aspects in establishing clinically reliable bone attachments.[1–4] To confer the roughness to dental implants, several methods can be used, such as electrochemical deposition, shot-blasting with abrasives, acidic etching, or combinations of such treatments. The cell adhesion, proliferation, and differentiation results from in-vitro studies suggest there is a positive correlation between surface roughness and cellular attachment and osteoblast-like cell activity.[1,3–5]

Together with the surface roughness, the design of a dental implant must always take into consideration the fatigue behavior that the implant will undergo through its lifetime. The fatigue limits of the materials used will have a key role when estimating the long-term performance of the implant. Thus, the assessment of the fatigue behavior of implantable alloys has acquired great importance.[6–8] In general, failures of dental implants are produced within the first 2 weeks of the surgery (85%), which can be caused by infection, low osseointegration capacity, increase of bone temperature produced by the drills, or poor bone quality, among others. The remaining 15% of the total failures are produced after 6 years of the surgery, when the implant has been integrated in the bone for a long time. In this case, the failures can be produced by peri-implantitis (10%), fatigue failures (4%), or

[1] Master de Implantología, Facultad de Odontología, Universidad de Sevilla, Spain.
[2] Dept. Ciència dels Materials i Enginyería Metal.lúrgica, E.T.S. Enginyeria Industrial, Universitat Politècnica de Cataluña, Barcelona, Spain.
[3] School of Dentistry, Universitat Internacional de Catalunya, Barcelona, Spain.
* *Corresponding author,* e-mail: xavier.gil@uic.cat
DOI: 10.1563/aaid-joi-D-16-00088

other causes (1%). Consequently, fatigue life is a very important property to take into account when considering the long-term behavior of dental implants.[9–10]

Taken together, we consider surface roughness and long-term mechanical stability as two key parameters that need to be properly designed for future applications. Therefore, we hypothesize that the fabrication process and surface treatments can be optimized to obtain proper surface roughness and fatigue life. In turn, this could be translated into a higher ability to osseointegrate with natural bone, showing higher bone-to-implant contact and lower ability to remove the implant from its location. In this sense, the objective of this study was to correlate the roughness and topography with the residual stress to analyze different fatigue behaviors and in vivo osseointegration, which were analyzed by histomorphometric and pull-out tests for 4 different types of surface treatments. The analyzed surfaces are as-machined (CTR), acid-etching (AE), spark anodization (SA), and grit-blasted (GB) CP titanium dental implants.

Materials and Methods

Implants

A bar of commercially pure grade III titanium (cpTi, ASTMB348) was used to machine both screw-shaped implants for histometric analysis and cylinders for pull-out tests. The screw-shaped dental implants were 3.8-mm diameter and 12.0-mm length with a 1.0-mm pitch and a 1.5-mm long collar (Figure 1). The cylinders were 3.8 mm in diameter and 10.0 mm in length, and had a 1.4-mm diameter transversal threaded hole to adjust the pull-out fixture while performing the mechanical tests.

Surface treatments

CP Ti implants and cylinders were prepared with four different surface treatments and divided into 4 groups with 16 implants and 10 cylinders per group:

- CTR,
- AE in 0.35-M hydrofluoric acid for 15 seconds at room temperature,
- SA in HCl 0.5M with a voltage of 320 V, and
- GB with alumina particles (600-μm) with 0.25 MPa blasting pressure until achieving roughness saturation.

Galimplant (Sarria, Spain) provided different types of Ti materials subjected to surface modifications. After surface treatments were performed, all implants were ultrasonically cleaned in soap and distilled water for 10 minutes, dried with nitrogen gas, and sterilized in ethylene oxide at 37°C and 760 mbar for 5 hours. Then, implants were aerated for 42 hours before being packed for surgery. Sterilization and packing of all implants was carried out at Aragogama S.L.

Surface roughness and topography

Roughness was evaluated in the framework of the recommendations by Wennerberg and Albrektsson[11] on topographic evaluation for dental implants. A white light interferometer

Figure 1. Representative scheme of the experimental titanium dental implant used.

microscope (Wyko NT1100, Veeco) was used. The surface analysis area was $189.2 \times 248.7\ \mu m^2$ for the smooth CTR surfaces and $459.9 \times 604.4\ \mu m^2$ for all the microrough surfaces. Data analysis was performed with Wyko Vision 232TM software (Veeco, Oyster Bay, NY). A Gaussian filter was used to separate waviness and form from the roughness of the surface. Cut-off values, $\lambda_c = 0.8$ mm, for CTR, AE, GB, SA surfaces and $\lambda_c = 0.25$ mm for CTR surfaces were applied, according to previous tests 5. The measurements were made in 5 different surfaces of each type of surface treatment to characterize the amplitude and spacing roughness parameters of average roughness (Ra) and peaks (Pc), respectively. Ra is the arithmetic average of the absolute values of the distance of all points of the profile to the mean line. Pc is the number of peaks in the profile per length of analysis. Ra and Pc were calculated by averaging the values of all individual profiles that were evenly distributed along the analyzed surface.

A scanning electron microscope (SEM) (JSM 6400, Jeol, Japan) was used to qualitatively analyze the surface topography of the implants before being implanted.

Mechanical properties

Residual stresses were measured for 5 dental implants for each group with a diffractometer incorporating a Bragg-Bentano configuration (D500, Siemens, Germany). The measurements were done for the family of planes (213) that diffracts at $2\theta = 139.5°$. The elastic constants of Ti at the direction of this family

Table 1

Chemical composition of artificial saliva

Chemical product	Concentration (g/dm^3)
K_2HPO_4	0.20
KCl	1.20
K S CN	0.33
Na_2HPO_4	0.26
NaCl	0.70
$NaHCO_3$	1.50
Urea	1.50
Lactic acid	until pH = 6.7

of planes are EC = (E/1+ν)(213) = 90.3 GPa.[1,4] The position of the peaks was adjusted with a pseudo-Voigt function using appropriate software (WinplotR, free online access), and then converted to interplanar distances using Bragg's equation.

Ten tensile specimens for each group with a ratio diameter to gauge length of 1/5, and fatigue specimens were machined. These were tested in a universal screw-driven testing machine (Bionix, MTS, Eden Prairie, Minn) of 100 kN capacity at a cross-head speed of 1 mm/min. The fatigue specimens (40 dental implants for each group) were cyclically deformed in tension-compression under strain control Re = −1 in a servohydraulic testing machine of 100 kN capacity. In order to mimic the conditions once implants are placed in patients, we performed the studies using a container with artificial saliva at 37°C. The chemical composition of the artificial saliva used is shown in Table 1. The strain rate was always kept constant at 6.5×10^{-3} s^{-1}. The total strain amplitude used was $\pm 7 \times 10^{-3}$. The deformed and fractured specimens were observed by means of SEM.

Animals

All animal handling and surgical procedures were conducted according to European Community guidelines for the care and use of laboratory animals (DE 86/609/CEE) and approved by the local veterinary school ethical committee and the Medicine School ethical committee of the Universitat Internacional de Catalunya (UIC-122015). A total of 40 implants were used, divided into four groups of 10 specimens according to their different surface characteristics as previously detailed.

For each time interval, 5 specimens were implanted. Twenty female adult New Zealand White rabbits (3.5 kg b.w., Charles River, Saint Aubin les Elboeuf, France) were operated under general anesthesia performed by intramuscular injections of xylazine (5 mg/kg) and ketamine (35 mg/kg). After lateral bilateral knee arthrotomy, a drilled bone defect of 4 mm in diameter and 6 mm deep was centered on the lateral condyle. The cavity was thoroughly rinsed with physiological saline. Implants were randomly carefully inserted into the defects. The wound was sutured in three layers. The rabbits were euthanized under general anesthesia at 4 or 10 weeks after implantation by an intracardiac injection of barbiturate (Dolethal s, Vetoquinol, France).

Histological preparation and histomorphometrical analysis

Femoral condyles were harvested, and peripheral soft tissue was removed. The samples were radiographed to localize the implant. Specimens were fixed for 7 days in 4% formaldehyde neutral solution rinsed in water, dehydrated in graded series of ethanol (from 70–100%) and embedded in polymethyl methacrylate. Each implant was longitudinally sectioned in the middle with a diamond circular saw (Leica SP1600, Wetzlar, Germany). After polishing and sputter coating with gold–palladium, the surfaces of the blocks were observed by SEM (Leo 1450VP, Hamburg, Germany) using the backscattered electrons (BSE) mode at a magnification of 15. The BSE mode made it possible to determine the titanium implant, host, and newly formed mineralized bone based on their gray levels. Global histomorphometry was carried out using a custom-made program developed in an image processing system (Quantimet 500MC, Leica, Cambridge, UK). The percentage of direct contact between mineralized bone and titanium surface was calculated using a semi-automatic binary treatment on each image. Bone growth was also determined inside the 4 chambers of the customized implants. The other part of the block was processed for histology. Approximately 100-mm–thick sections were made using a diamond saw (Leica SP1600).

The sections were then ground to a final thickness of about 50 mm. Qualitative examinations were performed by light microscopy on stained sections (1% methylenblue and 0.3% basic fuchsin).

Pull-out tests

The retrieved bones were mechanically stabilized during pull-out tests in a customized device. The setup was adjusted using a level tube to place the test area aligned with the load-cell. A threaded pin with a head was then fit in the pre-threaded hole of the implant. To minimize the effect of shear forces in the outcome of the mechanical test, a 350-mm–long wire with high rigidity (piano wire) was connected to the load-cell and the pinhead. Five cylinders were tested for each time (4 and 10 weeks) and for each group.

An Adamel (MTS) mechanical testing machine fitted with a calibrated load-cell of 1000 N was used to perform the pull-out tests. Cross-head speed range was set to 1.0 mm/min. Force measuring accuracy was ±1%. The load was recorded until loosening of the implant and plotted as load vs time. The maximum load during the test—that is, the retention value—is reported in this work to compare mechanical stability of the implants with different surface finishing.

Statistical analysis

Statistically significant differences among test groups for both histometry and mechanical evaluation were assessed using statistical software (Minitab 13.1, Minitab Inc, State College, Pa). ANOVA tables with multiple comparison Fisher's test were calculated. The level of significance was established at $P < .05$.

Standard deviations of the test groups and concordance correlation coefficient, λ_c, for assessing the reliability of the examiner were also calculated. λ_c ranges between 0 and 1, with values close to 1 indicating high reliability. In this study, the calculated λ_c was 0.98.

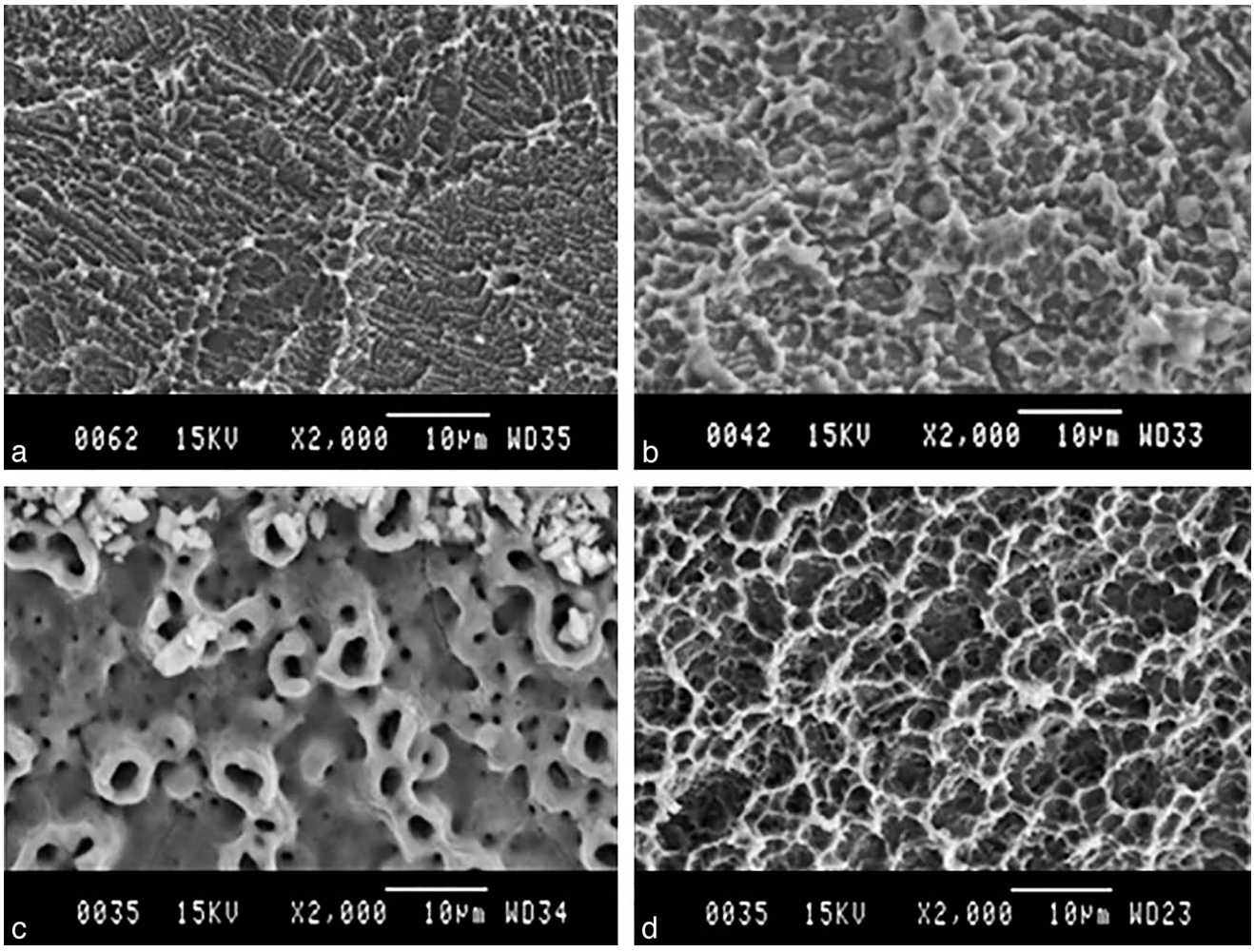

Figure 2. Scanning electron microscopy images of (a) as-received (CTR), (b) acid-etched, (c) spark-anodization, and (d) grit-blasted surface. As can be noted in the images, the different treatments provided significant differences in topography, presenting a slightly rough surface for the CTR, with similar morphology to AE although with slightly higher roughness. Further, the SA implants presented a considerable difference, a porous structure due to the electrochemical reaction and the hydrogen scape. Finally, the GB surfaces presented the highest roughness with similar morphological features to AE and CTR.

Results

Surface roughness

Initially, we analyzed the surface morphology and roughness of the different treatments. Figure 2 shows the microstructure of the surface treatments observed by SEM. The acid-etched surfaces were characterized by a myriad of small craters and grooves. The walls of the craters presented a micropatterned structure and pitting at the bottom of the craters. The Spark anodized presented a porous titanium oxide on the surface. The pore morphology was formed by the scape of hydrogen in the form of gas during the electrochemical reaction. The blasted surfaces had a heterogeneous surface structure with peaks and valleys of varied geometry showing several flat facets. The facets also had small irregularities appearing as pits and stripes.

We then analyzed the surface roughness with the profilometer. As expected, the shot-blasted specimens presented statistically significant ($P < .001$; Student's *t*-test) higher values of surface roughness than the CTR, AE, and SA. There were no significant differences in Ra values between AE and SA.

Residual stresses

Figure 3 confirms the compressive character of the residual stresses. As expected, the compressive stresses induced by grit blasting were statistically significant ($P < .001$; Student's *t*-test) and highly different from those induced on CTR, AE, and SA samples. There were no statistically significant differences between these three treatments.

Fatigue

Figure 4 shows the number of cycles to failure (N_f) and the cumulative plastic strain (ε_{cum}) for the different dental implants. It can be observed that the as-machined microstructure of the GB implants present longer life fatigue than did the CTR, AE, and SA. In addition, the CTR samples presents better fatigue behavior than the SA and AE.

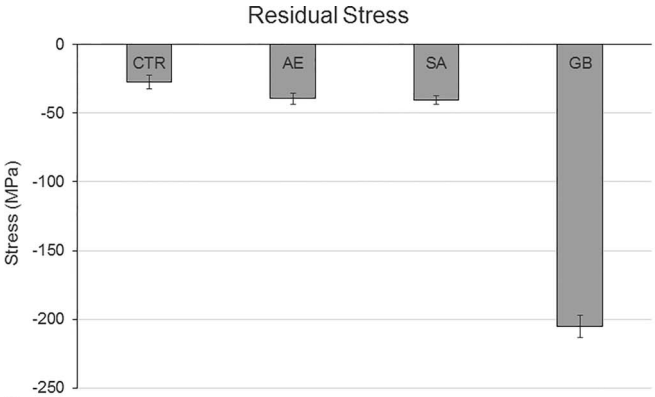

3

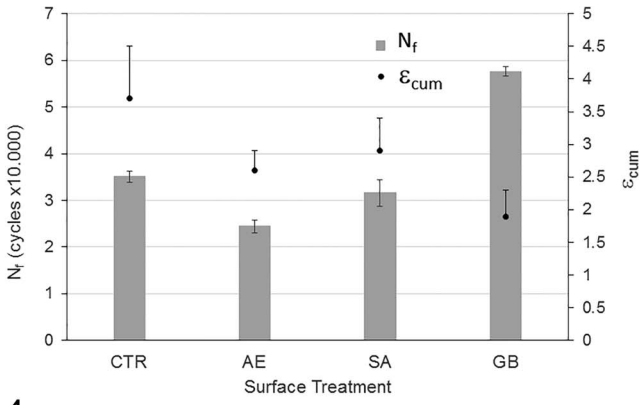

4

Figures 3 and 4. Figure 3. Surface residual stresses calculated at the 4 different types of Ti dental implant surfaces, showing that the grit-blasted surface (GB) treatment provided the higher residual stress, whereas the other treatments provided similar residual stresses to that of as-received (CTR) samples. **Figure 4.** Fatigue test results, showing the number of cycles needed for failure (Nf) (left axis) and the cumulative plastic strain (ε_{cum}) (right axis) for the different treated surfaces. AE indicates acid-etched; SA, spark-anodization.

In vivo osseointegration

Figure 5 shows representative histologies at each period of implantation for CTR, AE, SA, and GB, implants, respectively. Qualitatively, the histological images show an increased amount of bone-to-implant contact from 4 weeks to 10 weeks for all the studied samples, clearly showing the ability to completely or partially induce the formation of new bone. As expected, a higher surface roughness induced a higher amount of BIC area, demonstrating its higher ability to attract osteoblasts to start bone remodeling. The results were then quantified by histomorphometric analysis (Figure 6), clearly showing significantly higher values for the GB samples after 4 and 10 weeks of implantation.

Together with the BIC percentage, the pull-out test provided information on the strength needed to remove the implant from the bone. Figure 7 summarizes the retention values for the differently treated cylinders after 4 and 10 weeks of implantation. As shown with the BIC values, retention values also increased from 4 to 10 weeks. The values were highest for the GB groups. The most mechanical retention were GB implants corresponding at the maximum levels of osseointegration.

Discussion

Roughness and topographical features are the most relevant of the surface properties for a dental implant for its clinical success.[12] For that reason, we studied the surface topography

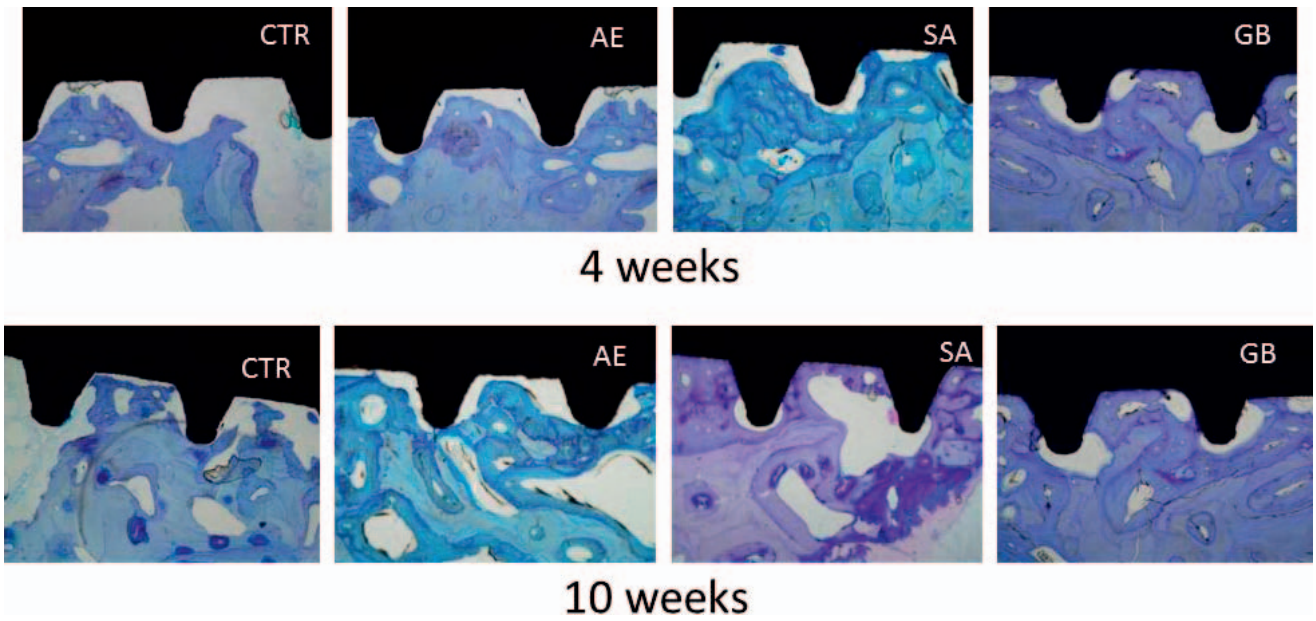

Figure 5. Representative histological images of as-received (CTR), acid-etched (AE), spark-anodization (SA), and grit-blasted surface (GB) implants after different times of implantation (4 weeks and 10 weeks). Bone remodeling is present in all cases, presenting as light color in the new bone formation and as dark color in the old bone. Especially for AE and GB, new bone is in close contact with the implant.

TABLE 2

Surface roughness of the different surface treatments. Results shown as mean ± standard*

Implant Surface	R_a (μm)	P_c (cm^{-1})
CTR	0.33 ± 0.1	150.9 ± 69
AE	1.69 ± 0.1	198.3 ± 34
SA	1.74 ± 0.2	82.1 ± 10
GB	3.43 ± 0.4	92.1 ± 13

*R_a indicates average roughness, the arithmetic average of the absolute values of the distance of all points of the profile to the mean line; P_c, number of peaks in the profile per length of analysis; CTR, as-received; AE, acid-etched; SA, spark-anodization; GB, grit-blasted surface.

(Figure 2) and surface roughness (Table 2) properties of the implants. GB surfaces were significantly rougher than SA, AE, and CTR surfaces, and AE surfaces were significantly rougher than CTR in comparison with others.[13–17] It is generally agreed that topography affects the cellular interaction, which influences the orientation, migration, growth, and differentiation of adhering cells.[18,19] Several in vivo studies have shown that surface roughness improves the osseointegration of Ti implants.[2,20] More specifically, in our view, this interaction is strongly influenced by the organization of surface-associated adhesive proteins such as fibronectin,[21–24] which in turn are expected to be dependent on the roughness and other associated physicochemical properties, such as residual stress. These parameters affect others, including wettability, surface energy, and surface charge. We anticipate that the third dimension of topography, which will affect the distribution of FN, may resemble the natural organization of ECM to a certain extent and will thus constrain the biological response.[18] Fibronectin is one of the key proteins involved in cell-biomaterial interaction[25] and has also been shown to play a distinct role in early bone development[26–27] and osteoblast differentiation.[18]

Taking into account that bone regeneration takes place by the deposition of new bone by osteoblasts, it is wise to think that overall bone regeneration ability will be dictated by the previously described surface properties of the materials. In this sense, our hypothesis is that the enhanced roughness and residual stress values can enhance the bone remodeling ability, thereby enhancing the dental implant's osseointegration into the site of defect. Due to the inherent benefits of a more stable and robust bonding between the bone and the implant, the current work describes the optimum combination for optimum bone to implant contact and stability.

For this reason, it is important to initially properly characterize the surface properties of the implant as well as the implant life depending on the treatment provided. The fatigue behavior of the samples submitted to shot-blasting treatment is better due to the compressive effect of the residual stresses on the surface that makes the crack nucleation difficult. This fact can be observed for the GB samples, where the crack grows from the surface and from 15 μm beneath the surface. As a consequence, an improvement of the fatigue behavior of the grit-blasted treatment is obtained. Consequently, GB treatment increases the implant surface roughness by impingement, at high pressure, of abrasive particles, resulting in local plastic strain. Although the variables of the grit-blasting treatment are not exhaustively controlled, the value of the residual compressive stresses on the surface layer, affected by the treatment, provokes the crack nucleation site to change from the specimen surface (for the CTR) to the specimen interior (for the GB). This change is postulated to result in a significant increase of fatigue properties of dental implants made of CP Ti.

That said, CTR and GB present better fatigue life than AE and SA. These treatments require high concentration of hydrogen (pH = 1–3) and can provoke the incorporation of this hydrogen into the titanium, producing the formation of titanium hybrids that are known to be brittle, which in turn reduce the fatigue life of the implants.[28,29]

From the histology results, only GB surfaces showed new mature bone formation around the dental implants after 4 weeks of implantation. This provided good primary stabilization

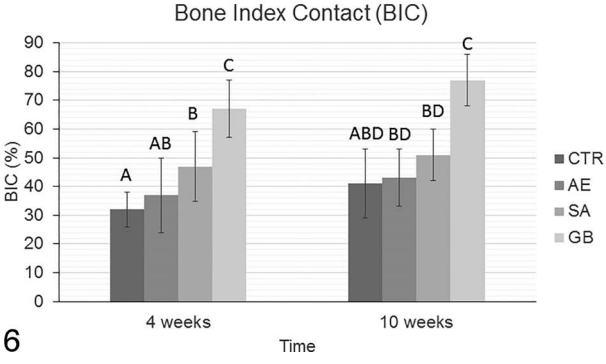

6

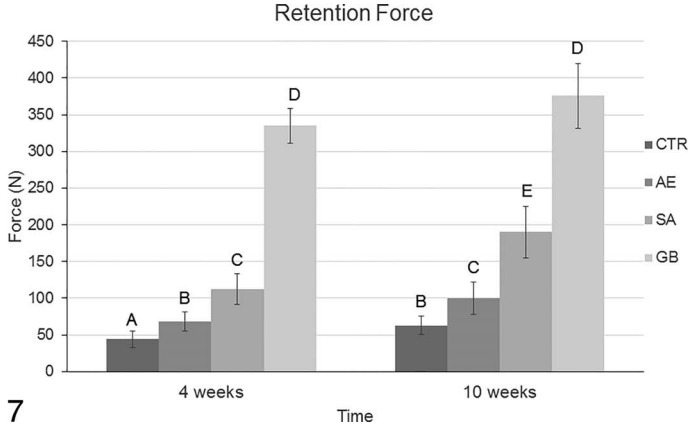

7

FIGURES 6 AND 7. FIGURE 6. In vivo animal study quantification of bone index contact (BIC) of the different types of surfaces, showing significant increased values for the GB samples. Columns with the same letter indicate no significant differences among the different groups and studied time points ($P < .05$). FIGURE 7. Retention force of the implants implanted in the rabbit condyle, showing the strength needed to pull the implants from the bone for the different surface treatments at the two different time points. Columns with the same letter indicate no significant differences among the different groups and studied time points ($P < .05$). CTR indicates as-received; AE, acid-etched; SA, spark-anodization; GB, grit-blasted surface.

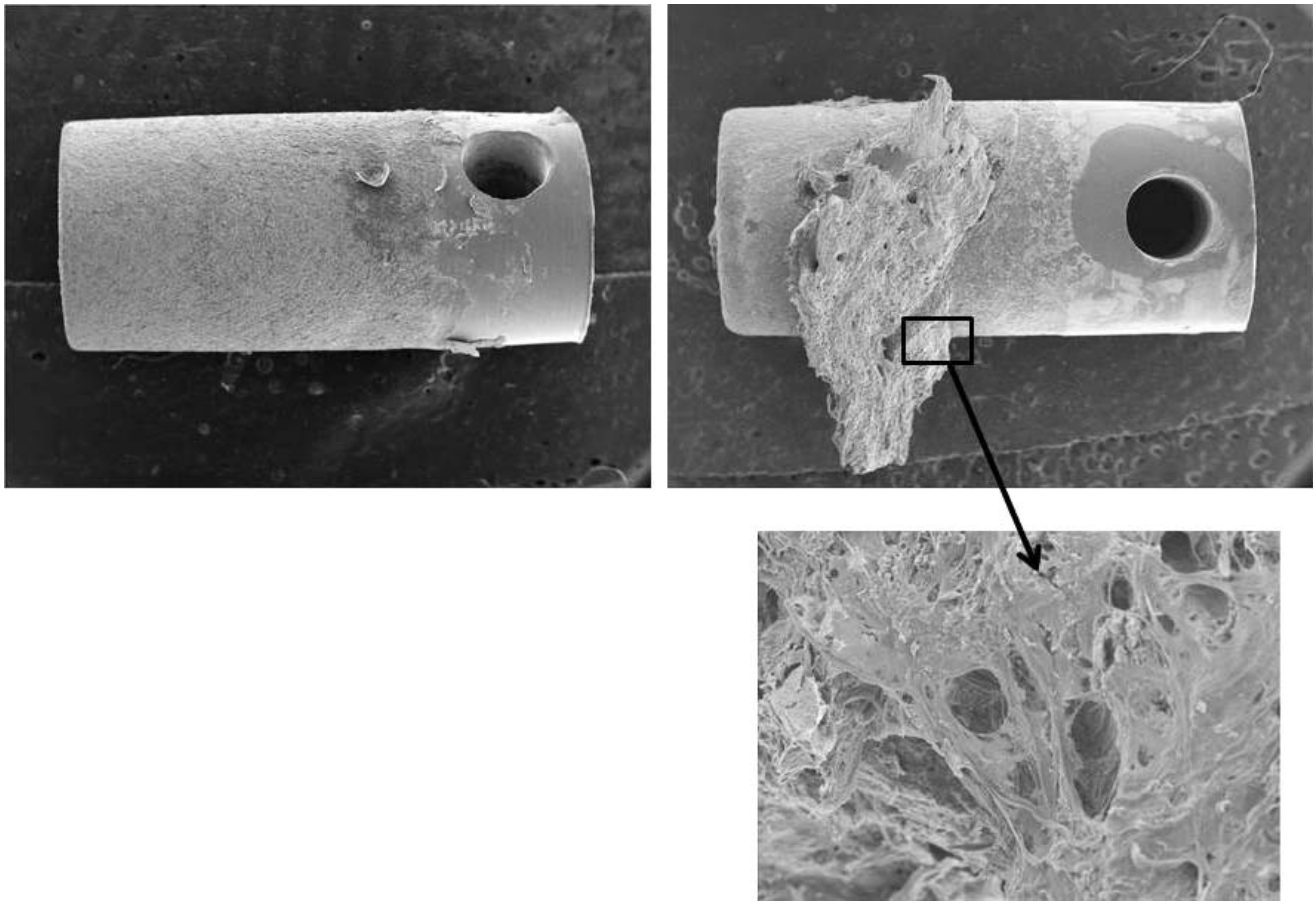

Figure 8. Pull-out tests. Cylinder-shaped implants after pull-out tests: (a) acid-etched implant and (b) grit-blasted surface implant with an attached piece of the surrounding bone tissues.

to all implants, even before the hard tissues started to significantly regenerate. The highest BIC was near 60% after 4 weeks of implantation in GB surfaces, confirming our previously discussed qualitative evaluation of the regenerated bone. GB implants had a significantly higher BIC than CTR, AE, and SA implants for almost all periods of implantation, including 10 weeks, which can be attributed to the effect of the optimized roughness for those types of implants.[30]

In this study, the evolution of the regeneration of bone around different types of implants qualitatively showed that the blasted surfaces with roughness $R_a \approx 4$ μm evidenced that GB had faster tissue colonization than CTR, AE, and SA surfaces.

The results of mechanical retention confirmed most of the results obtained for BIC. GB cylinders had significantly higher retention values than did CTR, SA, and AE cylinders in both periods of implantation. The mechanical retention of SA and AE cylinders was significantly higher than the CTR surfaces. This set of results suggested that the surface roughness at the microlevel is the main variable affecting mechanical retention at the periods of implantation studied. The effect of roughness on mechanical retention was assessed even at short implantations times, when the tissues were far from being fully regenerated around the implants—as in the case of AE cylinders after both 4 and 10 weeks of implantation. It was also notable that during the pull-out tests, parts of bone remained attached to the surfaces of some GB cylinders (observed in Figure 8). This same occurrence did not happen when CTR or AE cylinders were tested.

In summary, we have seen that the higher the roughness, the higher the retention of the implants. However, Ronold et al[31] showed that implant surface roughness higher than Ra ≈ 5.0 mm resulted in a decrease in their functional attachment. Thus, both GBlast have optimized roughness presented better fatigue and osseointegration behavior, as has been confirmed by our results.

Conclusions

Grit-blasting treatment increases the implant surface roughness by impingement, at high pressure, of small abrasive particles, which results in local plastic strain. This fact will produce a firmer and earlier fixation and a better osseointegration. The residual compressive stresses on the surface layer affected by the treatment provokes the crack nucleation site to change from the specimen surface to the specimen interior, increasing the fatigue life. GB implants show the best values of the BIC due to the roughness and, consequently, this treatment presents the best values of the bone attachment in the pull-out tests. The current results have may have great potential in the design of future implants, although future studies need to

be directed in controlling a more homogenous surface of the implant and test them in bigger animal models, such as a pig, which can be considered closer to humans. Furthermore, another limitation of the study was the site of implantation due to the size of the animal, which in future can be overcome by using the pig model and implantation in the mandible to allow observing the implants' performance in the theoretical site of implantation.

Abbreviations

AE: acid etching
CTR: implant as-received
GB: grit-blasted surface
SA: spark-anodization
SEM: scanning electron microscope

Acknowledgment

The authors are grateful to the Spanish government for the CICYT MAT-2015-67183-R (MINECO/DEFDER,UE).

References

1. Albrektsson T, Brånemark P-I, Hansson H-A, Lindström J. Osseointegrated titanium implants. Requirements for ensuring a long-lasting direct bone-to-implant anchorage in man. *Acta Orthop Scand*. 1981;52:155–170.

2. Buser D, Schenk RK, Steinemann S, Fiorellini JP, Fox CH, Stich H. Influence of surface characteristics on bone integration of titanium implants. A histomorphometric study in miniature pigs. *J Biomed Mater Res*. 1991;25: 889–902.

3. Giavaresi G, Fini M, Cigada A, et al. Mechanical and histomorphometric evaluations of titanium implants with different surface treatments inserted in sheep cortical bone. *Biomaterials*. 2003;24:1583–1594.

4. Ronold HJ, Lyngstadaas SP, Ellingsen JE. Analysing the optimal value for titanium implant roughness in bone attachment using a tensile test. *Biomaterials*. 2003;24:4559–4564.

5. Han CH, Johansson CB, Wennerberg A, Albrektsson T. Quantitative and qualitative investigations of surface enlarged titanium and titanium alloys implants. *Clin Oral Implant Res*. 1998;9:1–10.

6. Gil FJ, Aparicio C, Manero JM, Padrós A. Influence of the height of the external hexagon and surface treatment on fatigue life of commercially pure titanium dental implants. *Int J Oral Maxillofac Implants*. 2009;24:583–590.

7. Gil FJ, Espinar E, Llamas JM, Sevilla P. Fatigue life of bioactive titanium dental implants treated by means of grit blasting and thermochemical treatment. *Clin Implant Dent Relat Res*. 2014;16:273–280.

8. Gil FJ, Herrero M, Lázaro P, Rios JV. Implant-abutment connections: influence of the design on the microgap and their fatigue and fracture behavior of dental implants. *J Mater Sci Mater Med*. 2014;25:1825–1830.

9. Schwartz-Arad D, Kidron N, Dolev E. A long-term study of implants supporting overdentures as a model for implant success. *J Periodontol*. 2005; 76:1431–1435.

10. Thomsen P, Esposito M, Wictorin L, Aronsson B-O, Thomsen P. Bone response to machined cast titanium implants. *J Mater Sci Mater Med*. 1997; 8: 653–665.

11. Wennerberg A, Albrektsson T. Suggested guidelines for the topographic evaluation of implant surfaces. *Int J Oral Maxillofac Implants*. 2000;15:331–344.

12. Buser D. Titanium for dental applications (I). In: Brunette DM, Tengvall P, Textor M, Thomsen P, eds. *Titanium in Medicine*. Berlin: Springer Verlag; 2001:875–888.

13. Bagno A, Di Bello C. Surface treatments and roughness properties of Ti-based biomaterials. *J Mater Sci Mater Med*. 2004;15:939–945.

14. Cochran DL, Schenk RK, Lussi A, Higginbottom FL, Buser D. Bone response to unloaded and loaded titanium implants with a sandblasted and acid-etched surface: a histometric study in the canine mandible. *J Biomed Mater Res*. 1998;40:1–11.

15. Kokubo T, Kushitani H, Sakka S, Kitsugi T, Yamamuro T. Solutions able to reproduce in vivo surface-structure changes in bioactive glass-ceramic. *J Biomed Mater Res*. 1990;24:721–734.

16. Kokubo T. Bioactive implants [in Spanish]. *Anales de Química Int Ed*. 1997;93:49–55.

17. Wei M, Uchida M, Kim HM, Nakamura T. Apatite-forming ability of CaO-containing titania. *Biomaterials*. 2002;23:167–172.

18. Anselme K. Osteoblast adhesion on biomaterials. *Biomat*. 2000;21: 667–681.

19. Boyan BD, Lohmann CH, Dean DD, Sylvia VL, Cochran DL, Schwartz Z. Mechanisms involved in osteoblast response to implant surface morphology. *Ann Rev Mat Res*. 2001;31:357–371.

20. Larsson C, Esposito M, Liao H, Thomsen P. The titanium-bone interface in vivo. In: Brunette DM, Tengvall P, Textor M, Thomsen P, eds. *Titanium in Medicine*. Springer Verlag: Berlin; 2001:588–633.

21. Altankov G, Groth T. Fibronectin matrix formation by human fibroblasts on surfaces varying in wettability. *J Biomat Sci-Pol*. 1996;8:299–310.

22. Altankov G, Groth T. Fibronectin matrix formation and the biocompatibility of materials. *J Mat Sci Mat Med*. 1996;7:425–429.

23. Altankov G, Groth T, Krasteva N, Albrecht W, Paul D. Morphological evidence for a different fibronectin receptor organization and function during fibroblast adhesion on hydrophilic and hydrophobic glass substrata. *J Biomater Sci Polym Ed*. 1997;8:721–740.

24. Altankov G, Richau K, Groth T. The role of surface zeta potential and substratum chemistry for regulation of dermal fibroblasts interaction. *Materialwissenschaft und Werkstofftechnik*. 2003;34:1120–1128.

25. Garcia AJ. Get a grip: integrins in cell-biomaterial interactions. *Biomat*. 2005;26:7525–7529.

26. Nordahl J, Mengarelliwidholm S, Hultenby K, Reinholt FP. Ultrastructural immunolocalization of fibronectin in epiphyseal and metaphyseal bone of young-rats. *Calcif Tissue Int*. 1995;57:442–449.

27. Globus RK, Doty SB, Lull JC, Holmuhamedov E, Humphries MJ, Damsky CH. Fibronectin is a survival factor for differentiated osteoblasts. *J Cell Sci*. 1998;111:1385–1393.

28. Gil FJ, Padrós A, Manero JM, Aparicio C, Nilsson M, Planell JA. Growth of bioactive surfaces on titanium and its alloys for orthopaedic and dental implants. *Mater Sci Eng C*. 2002;22:53–60.

29. Le Guehennec L, Soueidan A, Layrolle P, Amouriq Y. Surface treatments of titanium dental implants for rapid osseointegration. *Dental Mater*. 2007;23:844-–854.

30. Ivanoff CJ, Hallgren C, Widmark G, Sennerby L, Wennerberg A. Histologic evaluation of the bone integration of TiO2 blasted and turned titanium microimplants in humans. *Clinic Oral Implants Res*. 2001;12:128–134.

31. Ronold HJ, Lyngstadaas SP, Ellingsen JE. Analysing the optimal value for titanium implant roughness in bone attachment using a tensile test. *Biomat*. 2003;24:4559–4564.